Determination of the Short-Wavelength Propagation Threshold in the Collective Excitations of Liquid Ammonia

F. Sette,[1] G. Ruocco,[2] A. Cunsolo,[1] C. Masciovecchio,[3] G. Monaco,[1] and R. Verbeni[1]
[1]*European Synchrotron Radiation Facility, BP 220, F-38043 Grenoble Cedex, France*
[2]*INFM and Dipartimento di Fisica, Universitá di L'Aquila, I-67100, L'Aquila, Italy*
[3]*Sincrotrone Trieste, Area Science Park, I-34017, Trieste, Italy*

(Received 15 November 1999)

The dynamics structure factor $S(Q,E)$ of liquid ammonia ℓ-NH_3 at $T = 200$ K and at its vapor pressure has been measured by inelastic x-ray scattering (IXS) in the $1-15$ nm^{-1} momentum transfer (Q) range. Contrary to previous IXS studies on other associated liquids and glasses, in ℓ-NH_3 a large inelastic signal is observed up to $Q = 15$ nm^{-1}. This, enabling $S(Q,E)$ measurements as a function of Q at constant E transfer, allows us to demonstrate experimentally the transition from a propagating dynamics regime, where the acoustic excitation energy linearly disperses with Q, to a high-Q regime, where it is no longer possible to observe a dominant excitation in the $S(Q,E)$.

PACS numbers: 63.50.+x, 61.10.Eq, 78.70.Ck

The advent of the inelastic x-ray scattering (IXS) spectroscopy with meV energy resolution has widened the possibility to study collective atomic dynamics in disordered systems, such as liquids and glasses, in the momentum transfer (Q) region approaching the inverse of the interparticle separation, Q_o [1,2]. A common feature in studies of glasses, glass-forming systems, and molecular liquids is the observation of propagating collective modes up to a maximum Q transfer, Q_m, which is a relevant fraction of Q_o: $Q/Q_m = 0.1$–0.5 [1]. At Q_m the excitation width, $\Gamma(Q)$, becomes equal to the excitation energy, $\Omega(Q)$, and therefore the excitation spectrum becomes a featureless broadband. At Q larger than Q_m, in the systems studied so far, the increasing elastic component in the $S(Q,E)$ strongly hides the presence of an inelastic signal, often already difficult to detect at $Q = Q_m$. This experimental scenario casts different opinions on how well one can define a propagating collective excitation in the considered high-Q regime. There are in fact different interpretations which could depend on the specific model chosen to represent the $S(Q,E)$ and to derive the spectroscopic parameters [3].

In this Letter we report a study of the $S(Q,E)$ of liquid ammonia, ℓ-NH_3, a moderately hydrogen-bonded liquid. In this system, an inelastic signal is observed up to the highest investigated value, $Q = 15$ nm^{-1}, corresponding to $Q/Q_o \approx 0.75$. Moreover the experimental determination of the $S(Q,E)$ as a function of Q for three different values of energy transfer E shows the following characteristic features: (i) negligible intensity at low Q, (ii) a well defined Brillouin line for small values of E, which gets increasingly broader and then disappears with increasing E, and (iii) a Q- and an E-independent plateau at Q values above the Brillouin peak position. These data give a qualitative but *model-independent* picture of the short-wavelength dependence of the Brillouin line in a disordered system: specifically, it shows that the observed modes lose their *plane-wave* character with increasing energy transfer. This qualitative analysis confirms similar results previously obtained on different systems such as simulated glasses [4,5]. Further on, the $S(Q,E)$ vs E is measured at different constant Q values and is put on an absolute scale. This allows us to reconstruct the $S(Q,E)$ vs Q at selected constant E values: this analysis confirms the direct measurements, and, most importantly, it allows us to observe a crossover from a dynamic regime characterized by the presence of the Brillouin line to one where this feature can no longer be observed; this transition takes place at a crossover momentum, Q_c, which turns out to agree quantitatively with the value, Q_m, derived using the damped harmonic oscillator (DHO) model [6] to represent the $S(Q,E)$ of this system.

The experiment has been carried out at the very high energy resolution IXS beam line ID16 at the European Synchrotron Radiation Facility. The instrument consists of a backscattering monochromator and five independent analyzer systems, held one next to each other with a constant angular offset on a 7 m long analyzer arm. The utilized Si(11 11 11) configuration gives an instrumental energy resolution of 1.6 meV full width half maximum (FWHM) [2] and an offset of 3 nm^{-1} between two neighbor analyzers. The momentum transfer is selected by rotating the analyzer arm. The spectra at constant Q and as a function of E were measured with a Q resolution of 0.4 nm^{-1} FWHM. Those at constant E and as a function of Q were measured using the analyzer number two, which is provided of movable apertures. The Q resolution was set to 0.2 nm^{-1} FWHM for $Q \leq 4$ nm^{-1}, and to 0.4 nm^{-1} FWHM for $Q \geq 4$ nm^{-1}. The E scans at constant Q were performed by varying the monochromator temperature with respect to that of the analyzer crystals. The Q scans at constant E were performed by setting a constant temperature offset between the monochromator and the second analyzer crystal and by rotating the analyzer arm to vary the scattering angle. Each spectrum, either at constant Q or E, took about 150 min, and each fixed-Q or fixed-E point was obtained by typically averaging five scans. The data were normalized to the intensity of the incident beam. The liquid sample was obtained by condensation *in situ* of high purity ammonia in a stainless steel cell held at $T = 200$ K in a cryostat and with ≈ 4 cm^3 volume. The cell and cryostat were operated in a vacuum chamber, mounted on the sample diffractometer. The x-ray beam passed through two 50 μm thick Kapton windows with a 6 mm diameter aperture. The sample length along the x-ray beam was 20 mm. The transverse dimensions of the focused x-ray beam were 0.15×0.3 mm^2.

The evolution as a function of Q of the IXS spectra representing the $S(Q,E)$ vs E is exemplified in Fig. 1 for the 2.8–14.8 nm^{-1} Q range. An inelastic signal can be clearly observed at the two sides of the quasielastic line, which is the main feature centered at $E = 0$ and aligned with the experimentally determined energy resolution function. Each one of these five spectra has been measured with one of the five analyzers, and the spectrum at 5.8 nm^{-1} was obtained with analyzer number two. The inelastic signal is structured at the low-Q values, and it becomes broad and featureless at the higher Q's, although it is still well visible on top of the tails of the quasielastic peak.

The spectra in the low-Q region have been analyzed following the same procedure used in previous work on liquid water. Namely, the $S(Q,E)$ data were fitted by the convolution of the experimentally determined resolution function with a model function made by the sum of a Lorentzian and a damped harmonic oscillator [2,7]. The Lorentzian accounts for the quasielastic contribution to the $S(Q,E)$ and the DHO for the two side peaks, whose energy position is $\Omega(Q)$ and width parameter is $\Gamma(Q)$. This fitting procedure gave good results up to $Q \approx 9$ nm^{-1}, and the dispersions of both $\Omega(Q)$ and $\Gamma(Q)$ are reported in Fig. 2. At the Q value $Q_m = 7.0 \pm 0.5$ nm^{-1} we observe that $\Omega(Q_m) \approx \Gamma(Q_m) = 13 \pm 3$ meV, and therefore for larger-Q values the collective modes become strongly overdamped. We also notice the basically linear dispersion of $\Omega(Q)$ corresponding to a speed of sound of 2600 ± 50 m/s, a value sensibly higher than the value of 2080 m/s found at low frequencies in the hydrodynamic limit [8]. This "fast sound" phenomenon resembles the similar effect found in liquid water. There, its thorough study has shown that the fast sound reflects the elastic behavior of the collective dynamics which comes out when the excitation frequency corresponds to a time scale shorter than that of the structural (α) relaxation process. In the water case, and this is very likely to be true also in ℓ-NH$_3$, the analysis of the shape of the $S(Q,E)$ by a viscoelastic approach in a broad temperature range has shown that the principal relaxation process responsible for the transition from the hydrodynamic to the "fast" value of the sound velocity is governed by a characteristic time, τ, whose activation energy is comparable to the hydrogen bond's energy [7,9]. In the case of liquid ammonia at low temperature, the fact that the sound velocity lies on the fully unrelaxed side at the investigated Q values strongly supports the use of the DHO analysis,

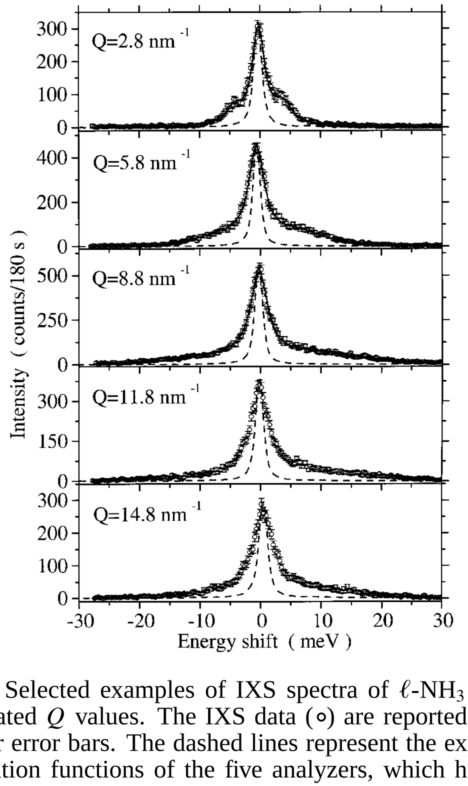

FIG. 1. Selected examples of IXS spectra of ℓ-NH$_3$ taken at the indicated Q values. The IXS data (∘) are reported together with their error bars. The dashed lines represent the experimental resolution functions of the five analyzers, which have been aligned with and scaled to the elastic peak. The full line on the three top spectra is the result of the DHO fit.

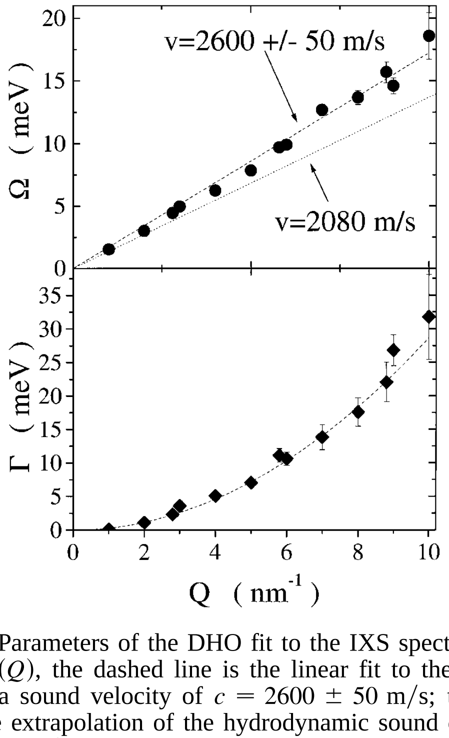

FIG. 2. Parameters of the DHO fit to the IXS spectra. Upper panel: $\Omega(Q)$, the dashed line is the linear fit to the data and indicates a sound velocity of $c = 2600 \pm 50$ m/s; the dotted line is the extrapolation of the hydrodynamic sound dispersion ($c_o = 2080$ m/s [8]). Lower panel: $\Gamma(Q)$, the dashed line is the quadratic fit to the data, $\Gamma(Q) = dQ^2$, with $d = 0.29$ meV nm^2.

being the DHO shape the expression for $S(Q,E)$ obtained in the viscoelastic framework in the $E\tau \ll \hbar$ limit. Finally, the $\Gamma(Q)$ shows a quadratic Q dependence, as found in the high frequency dynamics of all disordered systems studied so far [1].

The main points that have been questioned so far on the analysis of high-Q spectra in disordered systems as those presented here are (i) how much the results depend on the specific model chosen to represent the $S(Q,E)$, especially at Q values around and above Q_m, where the inelastic signal becomes very broad and almost hidden in the tails of the quasielastic peak, and (ii) what governs the evolution of a well defined Brillouin line into a broadband, and, in this respect, what could be the physical meaning of Q_m. One also has to consider that, in many of the systems previously studied, Q_m coincided with the highest-Q value where an inelastic signal could be observed at all.

Liquid ammonia, thanks to the clear observation of an inelastic signal below and above Q_m, seems to be an ideal system to investigate these points. Along this line, spectra were recorded as a function of Q and at four constant energy transfer values, E^*: $E^* = 0$, 5, 10, and 15 meV. These spectra are reported in Fig. 3, after normalization by an arbitrary intensity factor. The spectrum at $E^* = 0$ gives the Q dependence of the quasielastic line in the considered Q region and is shown here to demonstrate that this contribution to the spectra at $E^* \neq 0$ does not introduce artificial features, but it gives an almost Q-independent background. This allows a clean detection of the Brillouin peak at low E^*, contrary to the case in the $S(Q,E)$ vs E spectra, where this peak can be deduced only by a fitting procedure. This is evident at $E^* = 5$ meV, where the peak is centered at $Q^* = 2.8$ nm^{-1}, in agreement with the dispersion relation reported in Fig. 2. In the spectrum at $Q = 2.8$ nm^{-1} shown in Fig. 1, however, the energy position of the inelastic line ($E = 5$ meV) can be obtained only after the fit. These data, therefore, provide a direct experimental evidence of a Brillouin line in the considered high-Q region. With increasing energy, this peak moves towards a higher-Q value with a linear dispersion characteristic of propagating sound waves; it becomes increasingly broader and finally, at the highest-E^* value of Fig. 3, disappears leaving a "steplike" feature to mark its position and broadening.

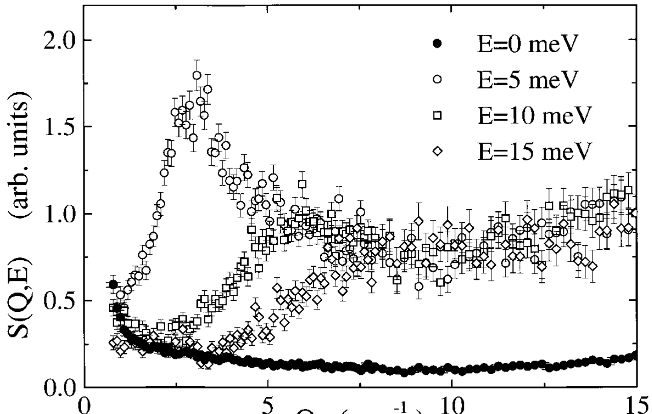

FIG. 3. IXS spectra, shown with error bars, taken as a function of Q at the indicated constant energies. The inelastic data (open symbols) have been normalized imposing similar values at $Q = 15$ nm^{-1}. The elastic spectrum (full symbol) has been normalized to the other spectra in the low-Q region.

The qualitative analysis of the IXS intensity measured at constant E cannot be pushed further. Few experimental artifacts, as well as the Q dependence of the molecular form factor, do not allow us to put the experimental data on an absolute intensity scale. On the contrary, the measurements taken at constant Q can be reported on an absolute scale, exploiting the first moment sum rule for $S(Q,E)$ [10], $\int ES(Q,E)\,dE = \hbar^2Q^2/2M$, to normalize the data. From the normalized spectra, measured on a dense Q grid, we have reconstructed the $S(Q,E)$ vs Q at constant E at the desired E^* values. The E^* has been chosen equally spaced ($\Delta E^* = 2$ meV) and, in order to improve the signal-to-noise ratio, the $S(Q,E)$ has been averaged over an energy range $\Delta E = \pm 1$ meV around the mean value E^*. These constant-E cuts of the $S(Q,E)$ are reported in Fig. 4, for selected E^*. These spectra confirm the findings of Fig. 3 and show the following general features: (i) the absence of intensity on the small Q side of the Brillouin peak, (ii) a

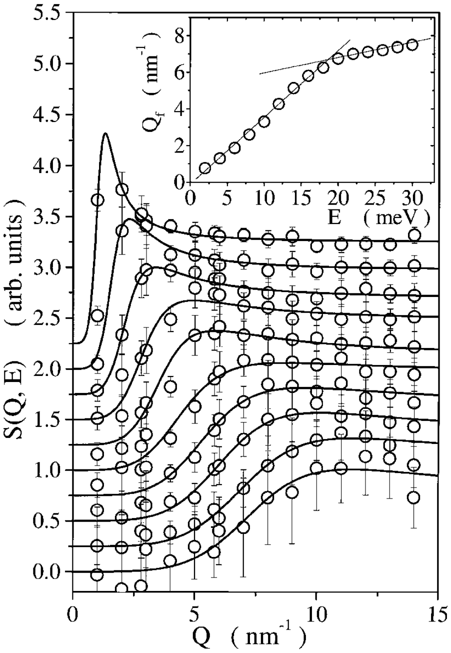

FIG. 4. Constant energy cuts of the $S(Q,E)$ reconstructed from the constant-Q cuts as explained in the text and normalized to their plateau value. The data (○), $E^* = 2$, 4, 6, 8, 10, 12, 14, 16, 20, 26 meV from top to bottom, are reported together with their error bars and their DHO best fit (full lines). The inset shows the E^* dependence of the inflection point Q_f (the Q value where the normalized spectra equal 0.5). The spectra are shown with a background increasing by 0.25 arbitrary units steps.

well defined Brillouin line for small values of E^*, which gets increasingly broader and then disappears with increasing E^*, and (iii) a plateau at Q values above the Brillouin peak position. Moreover, at high-E^* values, when the Brillouin peak is no longer visible, a step marks the transition from the zero intensity at low Q towards the plateau at high Q. The step position, Q_f, defined as the Q position where the $S(Q, E^*)$ is half the value of the plateau and determined by linear interpolation, is reported in the inset in Fig. 4. The position of this step changes with E^*, with a rate that is different in the low- and high-E^* limits. The linear extrapolation of Q_f allows us to find a threshold value, $Q_c \approx 7\ \mathrm{nm}^{-1}$, separating the low-$Q$ and high-Q behaviors. The low-Q behavior reflects the linear dispersion of the Brillouin line and, therefore, the persistence of a propagating collective dynamics. The almost constant high-Q behavior, on the contrary, confirms the transition towards a localized dynamical regime.

The determination of Q_c, independently from any specific model of $S(Q, E)$, allows a direct comparison with Q_m, the parameter obtained from the DHO analysis of the data of Fig. 1 and from the relation $\Omega(Q) = \Gamma(Q)$. We find that Q_c and Q_m are basically identical, and therefore this provides a strong indication that the DHO can give a good representation of the $S(Q, E)$ in liquid ammonia, and that the relation $\Omega(Q) = \Gamma(Q)$ can be used to define the threshold Q value where the sound waves change character. This observation is supported by the solid lines in Fig. 4, obtained using the DHO to fit the data. Here, the Q dependence of the parameters $\Omega(Q)$ and $\Gamma(Q)$ has been imposed using the functional forms $\Omega(Q) = \hbar c Q$ and $\Gamma(Q) = dQ^2$. The values of c, d, and that of an overall intensity factor have been left as E^*-dependent free parameters. The c values turn out to be E^* independent and coincide with the previously derived value $c = 2600$ m/s, while d is found to be larger than the value $d = 0.29\ \mathrm{meV\,nm}^2$ derived from Fig. 2b because of the increased energy broadening of the spectra reported in Fig. 4.

A final noteworthy implication of the data in Figs. 3 and 4 comes from the presence of the high-Q plateau, present even when one can observe a well defined Brillouin peak. This implies that, besides a dominant plane wave component with $Q(E^*) = E^*/\hbar c$, there is always a further relevant component at $Q \gg Q(E^*)$ which persists even at those high energies when the plane-wave character is lost. In this respect, it is particularly interesting to observe that the $S(Q, E)$, as shown in Fig. 4, has a striking resemblance to that found in model glasses [11,12]. Pushing this observation even further, one can relate the shape of the $S(Q, E)$ to the spatial pattern of the eigenmodes in disordered systems. In fact, as found in harmonic glass models [4], the plateau can be associated with the “random” component of the eigenvectors.

In conclusion, the study of constant-E and constant-Q cuts of the $S(Q, E)$ in liquid ammonia—a system with a large inelastic intensity at high-Q values—shows that it is possible to determine experimentally a threshold momentum which marks the transition between two dynamic regimes, characterized, respectively, by the persistence or lack of propagating sound waves.

We acknowledge B. Gorges for the construction of the ammonia cell.

[1] F. Sette, M. Krisch, C. Masciovecchio, G. Ruocco, and G. Monaco, Science **280**, 1550 (1998).
[2] G. Ruocco and F. Sette, J. Phys. Condens. Matter **11**, R259 (1999).
[3] For example, see *Proceedings of the VII Workshop on Disordered Systems*, edited by A. Fontana and G. Viliani [Philos. Mag. **77** (1998)].
[4] V. Mazzacurati, G. Ruocco, and M. Sampoli, Europhys. Lett. **34**, 681 (1996).
[5] S. N. Taraskin and S. R. Elliott, Phys. Rev. B **59**, 8572 (1999).
[6] B. Fak and B. Dorner, Institute Laue Langevin (Grenoble, France) Technical Report No. 92FA008S, 1992.
[7] A. Cunsolo, G. Ruocco, F. Sette, C. Masciovecchio, A. Mermet, G. Monaco, M. Sampoli, and R. Verbeni, Phys. Rev. Lett. **82**, 775 (1999); **82**, 2810(E) (1999).
[8] E. W. Lemmon, M. O. McLinden, and D. G. Friend, *Thermophysical Properties of Fluid Systems*, in NIST Standard Reference Database No. 69, edited by W. G. Mallard and P. J. Linstrom (NIST, Gaithersburg, MD, 1998).
[9] G. Monaco, A. Cunsolo, G. Ruocco, and F. Sette, Phys. Rev. E **60**, 5505 (1999).
[10] U. Balucani and M. Zoppi, *Dynamics of the Liquid State* (Clarendon Press, Oxford, 1994).
[11] M. Sampoli, P. Benassi, R. Dell’Anna, V. Mazzacurati, and G. Ruocco, Philos. Mag. **77**, 473 (1998).
[12] W. Goetze and M. R. Mayr, cond-mat/9910054.